Accepted Manuscript

Development of conductive paraffin/graphene films laminated on fluoroelastomers with high strain recovery and anti-corrosive properties

Luca Valentini, Silvia Bittolo Bon, Miguel-Angel Lopez-Manchado, Lorenzo Mussolin, Nicola Pugno

PII: S0266-3538(17)30559-6

DOI: 10.1016/j.compscitech.2017.06.023

Reference: CSTE 6819

To appear in: *Composites Science and Technology*

Received Date: 7 March 2017

Revised Date: 19 June 2017

Accepted Date: 21 June 2017

Please cite this article as: Valentini L, Bon SB, Lopez-Manchado M-A, Mussolin L, Pugno N, Development of conductive paraffin/graphene films laminated on fluoroelastomers with high strain recovery and anti-corrosive properties, *Composites Science and Technology* (2017), doi: 10.1016/j.compscitech.2017.06.023.

Development of conductive paraffin/graphene films laminated on fluoroelastomers with high strain recovery and anti-corrosive properties

Luca Valentini[1*], Silvia Bittolo Bon[1], Miguel-Angel Lopez-Manchado[2], Lorenzo Mussolin[3], Nicola Pugno[4,5,6]

1 Civil and Environmental Engineering Department, University of Perugia, UdR INSTM, Strada di Pentima 4, 05100 Terni, Italy.

2 Instituto de Ciencia y Tecnología de Polímeros, ICTP-CSIC, Juan de la Cierva, 3 28006 Madrid, Spain

3 Physics Department and SERMS Laboratory, University of Perugia, Strada di Pentima 4, 05100 Terni, Italy.

4 Laboratory of Bio-Inspired and Graphene Nanomechanics, Department of Civil, Environmental and Mechanical Engineering, University of Trento, Trento - Italy

5 School of Engineering and Materials Science, Queen Mary University of London, Mile End Road, London - United Kingdom.

6 Ket-Lab, Edoardo Amaldi Foundation, Italian Space Agency, via del Politecnico snc, I-00133 Roma, Italy

Abstract

Parafilm is a soft, solvent-proof and self-sealant thermoplastic material obtained by blending paraffin wax and polyolefin and that displays irreversible elongational thinning as the material is stretched. In this paper a lamination process was used to transfer graphene nanoplatelets (GNPs) on self-adherent Parafilm substrate and we show that a high-strain state of such conductive Parafilm/ GNPs film is reversible when the film is transferred by lamination to a fluoroelastomer (FKM) substrate. The stretching of GNP network stuck on viscoelastic Parafilm gave rise to regions of high and low GNP concentrations with increasing the electrical resistance upon stretching. Upon relaxation from a high-strain state, the composite film on FKM substrate maintain the initial electrical conductive state. Finally it was shown the reduction of the ethanol corrosion action in terms of swelling and mechanical performance of the neat FKM when the Parafilm/GNPs film is used for its packaging. In view of the low cost thermoplastic polymer used for the transferring and the lamination method propose, these findings represent a facile and an industrial scalable approach to realize novel multifunctional elastomer composites.

Keywords: graphene; fluoroelastomers; lamination; mechanical properties; stretchable conductors.

Introduction

Parafilm is the most used thermoplastic paraffin material in research laboratories as sealant plastic foil since it is resistant against many polar solvents. The Parafilm is hydrophobic, stretchable, soft and due to its low melting point it becomes adhesive applying heat during lamination, sticking strongly to the receiving substrates. The Parafilm utilization in several research fields is well known [1-5] and such material has received attention because it was used with success for transferring of few-layer graphene sheets by lamination [6]. Graphene flakes were embedded into paraffin wax to prepare graphene/wax composites with electromagnetic interference (EMI) shielding performance [7]. Recently, the combination of the stretchable and hydrophobic functionalities of Parafilm with the electrical conductivity of carbon nano-fibers was found advantageous for realizing printable electronics by spray coating method [8].

Unfortunately, Parafilm displays irreversible plastic deformation when stretched thus hindering its application for reversible stretchable electronic where high elastic recovery is required. The self-sticking properties of the Parafilm to adhere to stretchable substrates could be a viable and facile solution to make possible the high-strain recovery when the stress is released. A lot of examples of highly stretchable and conductive multifunctional materials have been reported in literature, with the most of them obtained by mixing a conductive percolation network of nanwires/nanoparticle within the host matrix making these methods matrix dependent for scalable applications [8,9-13].

Highly stretchable fluoroelastomers (FKM, typically containing 65% fluorine) with stretch ratios $\lambda>6$ (where λ = final length/initial length, or L_f/L_i) are of critical importance in solving problems in aerospace, automotive, chemical and petroleum industries [14,15]. In particular FKM materials are noted for their high resistance to heat and a wide variety of chemicals, other key benefits include excellent resistance to aging and ozone and very low gas permeability. However FKM materials are generally not resistant to ethanol, methanol and glycols fluids. Hence, new products of FKMs with enhanced performance is needed. The specific challenge in this regard is a quantified target

that consists in the optimization of elastomeric-like nanocomposites with multifunctional properties like monitoring the FKM strain with electrical resistance variation and anti-corrosion properties for the compatibility of such materials with high percentage of ethanol blended gasoline and with improved resistance to solvents.

Since the main factors that affect the composite properties are the particle size and the mode of interactions with the matrix materials, the nano-scale dimensions of 2D graphitic nano-inclusions such graphene nanoplatelets (GNPs) result in a huge benefit thanks to a better shape factor, larger contact surface and higher mechanical strength. It was found that the use of GNPs [16] ensures very good dispersion into the polymer phase and improves the most the mechanical and electrical properties of the composite, by enhancing the interface between the filler and the host medium. GNPs are very effective in improving the barrier properties of a polymer nanocomposite, by inhibiting the molecular diffusion through the matrix also resulting to enhanced corrosion resistance and low permeability [17,18].

Here we report a novel method that consist in the lamination of hydrophobic Parafilm containing graphene nanoplatelets (GNPs) on fluorelastomer substrate. Once laminated, the Parafilm/GNPs film maintains the electrical resistance reversible under stretch ratios up to λ=3. Finally, when the Parafilm/GNPs film is used as packaging medium of FKM, the fluoroelastomer exhibits improved mechanical and swelling properties against ethanol corrosion.

Experimental details

Graphene nanoplatelets (GNPs) were kindly supplied by NANESA (G3Nan average thickness of 9 nm $\sim$ 25 layers). GNPs were dispersed in chloroform at various concentrations ranging from 0.05

mg ml^{-1} to 1mg ml^{-1}. GNPs were dispersed for 15min at room temperature using a sonication bath with the power fixed at 80% and a frequency of 40 kHz. Commercially available glass has been used as substrate. The glass surface was cleaned with ethanol and acetone, rinsed with water, dried under nitrogen and taken inside a dry Ar glovebox. Afterwards, the glass surface was treated in oxygen plasma for 10 min. The plasma was generated by a radio frequency power supply (13.56 MHz) and carried out at room temperature with the gas pressure fixed at $4.5x10^{-2}$ Torr. The power employed was fixed at 20W (substrate bias 300 V). The GNP dispersion was drop on the glass substrate and left to evaporate the solvent at room temperature. Drop cast GNPs were then transferred to Parafilm film (Parafilm M®, Pechiney Plastic Packaging Company) through direct transfer process, which consists of lamination. The lamination provides the pressure necessary to achieve close contact between the GNPs and the Parafilm substrate so that the GNPs remain attached to the substrate. DSC was carried out in a TA Q200. Each sample was heated from 25 to 160°C at a heating rate of 10°C/min and then cooled at the same rate. Melting and crystallization temperatures, were determined from a subsequent heating run.

Fluoroelastomer (FKM), FC2122 used in this work is a dipolymer made from hexafluoropropylene and vinylidene fluoride that has an incorporated bisphenol cure system, which was kindly supplied by 3M^{TM} Dyneon. FKM compound was prepared in an open two-roll laboratory mixing mill (Comerio Ercole) at room temperature. The rotors operated at a speed ratio of 1:1.4. Rubber compound was vulcanized in an electrically heated hydraulic press (Gumix) at 177 °C and 200 MPa. The optimum cure time, t_{90} was previously determined by using a Monsanto Moving Die Rheometer MDR 2000E.

The Parafilm/GNP film was laminated on the FKM sheet at ~110°C. At this temperature the Parafilm becomes soft and sticky. The lamination was performed by using a cylindrical rod steel applying the pressure and temperature necessary to mould the Parafilm/GNPs film to the FKM substrate.

The samples, consisting of GNPs transferred to paraffin film and Parafilm/GNPs on FKM, were cut into strips of ~ 100 mm × 20 mm × 0.13 mm. The mechanical properties were measured by a universal tensile testing machine (Lloyd Instr. LR30K) with a 250 N cell at room temperature. The extension rate was 10 mm x min^{-1} and the gauge length was 60 mm.

At each elongation, or stretch ratios λ, of the Parafilm/GNPs and Parafilm/GNPs on fluoroelastomer samples, the electrical resistance was measured using a computer controlled Keithley 4200 source. The electrical resistance measurements were performed by biasing the Parafilm/GNP coating between two strips of silver paint located at a distance of 25 mm and perpendicular to the strain direction. Since the thickness and width of the substrate were found to decrease during the stretching, the resistance variation was calculated from the differential of the fundamental formula $d(R)=d(\rho l/A)$ as $dR/R=d\rho/\rho+dl/l-dA/A$ where R, ρ, l and A are the electrical resistance, the electrical resistivity, the length and the cross section area, respectively. Finally expressing $dA/A=-2\nu dl/l$, the resistance change can be written as $dR/R=d\rho/\rho+(1+2\nu)\varepsilon$ where ν and ε are the Poisson's ratio and the strain of the sample, respectively. Moreover, for our calculations, we assumed a Poisson's ratio of 0.4 for paraffin wax [19].

The morphology of the prepared samples was investigated by atomic force microscopy (AFM) and field emission scanning electron microscopy (FESEM, Zeiss Supra 25). AFM images were obtained operating in phase contrast tapping mode with a scanning probe microscope (Nanosurf easyScan DFM). Height and phase images were obtained under ambient conditions with a typical scan speed of 0.5 line/s, using a scan head with a maximum range of 70μm x 70μm.

Results and discussion

Parafilm is an inexpensive thermoplastic materials composed primarily of paraffin wax and polyolefin. In its solid form, the wax component is semicrystalline with low melting points (i. e. 50-

100°C). Parafilm shows large deformations when strained as reported in Fig. 1a. In particular, the strained Parafilm specimen shows a linear elastic zone followed by a plastic zone with downward slope before break.

The GNPs can be visually identified after the transfer procedure to the target Parafilm substrate, as shown in Fig. 1b. When the GNPs were transferred to the Parafilm film a mechanical response similar to neat Parafilm has been recorded (Fig. 1b) with higher strength and elongation at break (see Table I). This effect is well known in composites where stiff and soft phases coexist and the stiff phase reinforces and thereby strengthens the soft one [20-22]. The high stretch-ratio property of the underlying fluoroelastomer substrate is also reported in Fig. 1c. Parafilm is a thermoplastic material obtained by mixing paraffin wax and polyolefins with different molecular weight; DSC enables a determination of transition temperatures for these constituents as reported in Fig. 1d. The DSC heating curves for Parafilm and Parafilm/GNPs samples, respectively, show three endothermic peaks at about 45°C, 58°C and 99°C. The first two peaks are due to the melting crystalline wax fractions having different molecular weight distributions [23] while the peak at higher temperature is the polyolefin melting peak. Polyolefin and paraffin wax crystallization peaks were recorded during the cooling at 80ºC and 50°C, respectively.

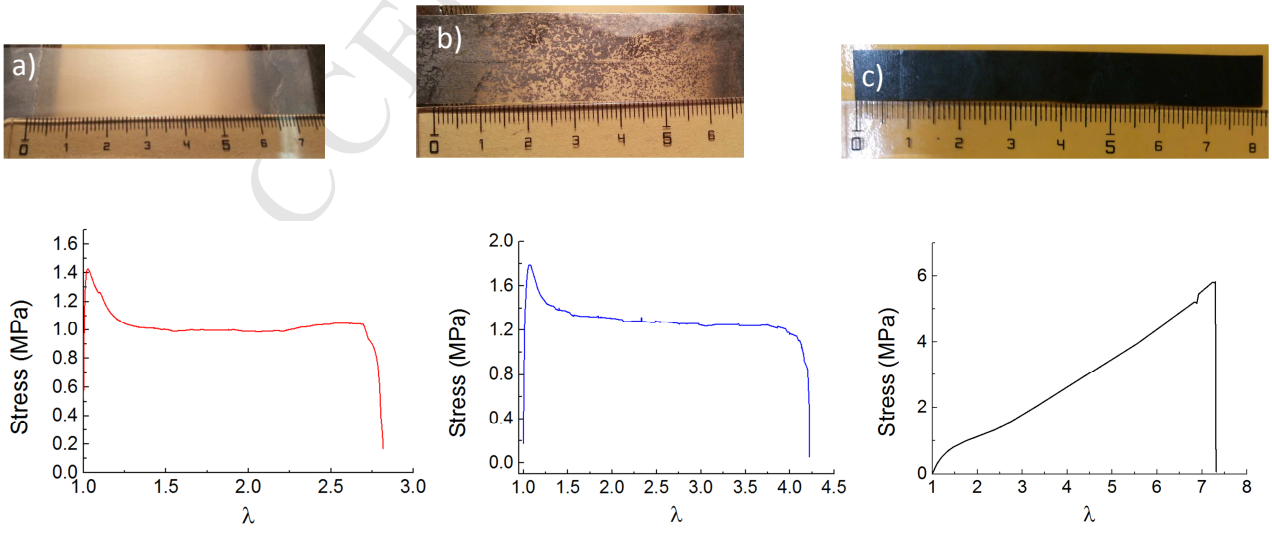

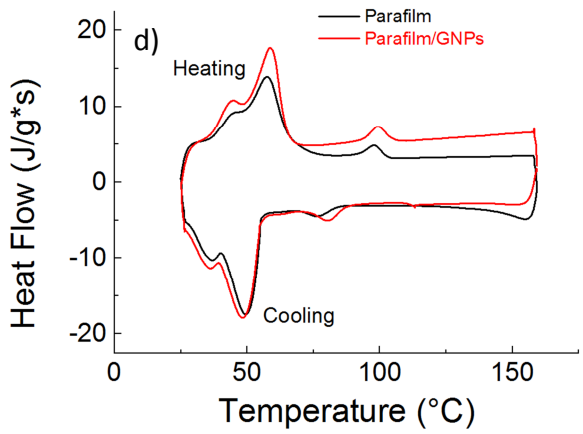

Figure 1. Photographs and stress-stretch ratio curves of (a) Parafilm, (b) Parafilm/GNPs and (c) FKM samples, respectively. (d) DSC heating/cooling curves of Parafilm and Parafilm/GNPs samples.

Table I. Average values and standard deviations of the mechanical characteristics and volume change after immersion in ethanol of three specimens of each prepared sample.

Samples	**Strength (MPa)**	**Elongation at break (%)**	**ΔV (%)**
Parafilm	1.0±0.2	157±20	-
Parafilm/GNPs	1.6±0.1	273±44	-
FKM	5.8±0.6	623±40	-
FKM after 48h in ethanol	4.2±0.3	458±45	14.16±0.08
FKM packed with Parafilm film after 48h in ethanol	3.5±0.3	536±38	1.66±0.03
FKM packed with Parafilm/GNPs film after 48h in ethanol	4.9±0.3	549±55	1.71±0.03

Interestingly, once transferred to the Parafilm tape and strained, the composite film shows the appearance of bands oriented orthogonal to the strain direction (Figures 2a and 2b). The formation of such bands is due to a plastic deformation and is reminiscent of a soft response that has been recently observed in liquid crystal elastomers, where, for example, if the material is deformed orthogonally to the alignment direction of the nematic phase, a short-range ordering has been reported [24]. The presence of such bands could be due to an uneven distribution of the GNPs within the material, which elongate more than the rest of the material. If this is the case, the macroscopic elongation measured would be a complex average of two different phases, with different mechanical properties. The local mechanical behaviour of two different phases was investigated by AFM analysis in phase contrast tapping mode. This non-invasive technique has been used to qualitatively map the films surfaces evidencing the contrast between the hard and the soft phases that are present on the film surface. Fig. 2c shows the AFM picture recorded on Parafilm/GNP coating after stretching; the region outside the band is characterized by a different surface morphology (Fig. 2c) with the presence of an hard phase dispersed into a soft polymer matrix outside the shear band can be distinguished. When passing to the plastic band, microcracks appeared, as illustrated in Fig. 2c. This finding can be explained suggesting that stretching such viscous substrate gave rise to inhomogeneous density distributions of GNPs with mesoscopic size that are dragged away upon stretching.

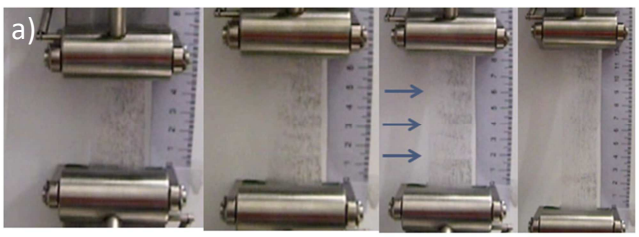

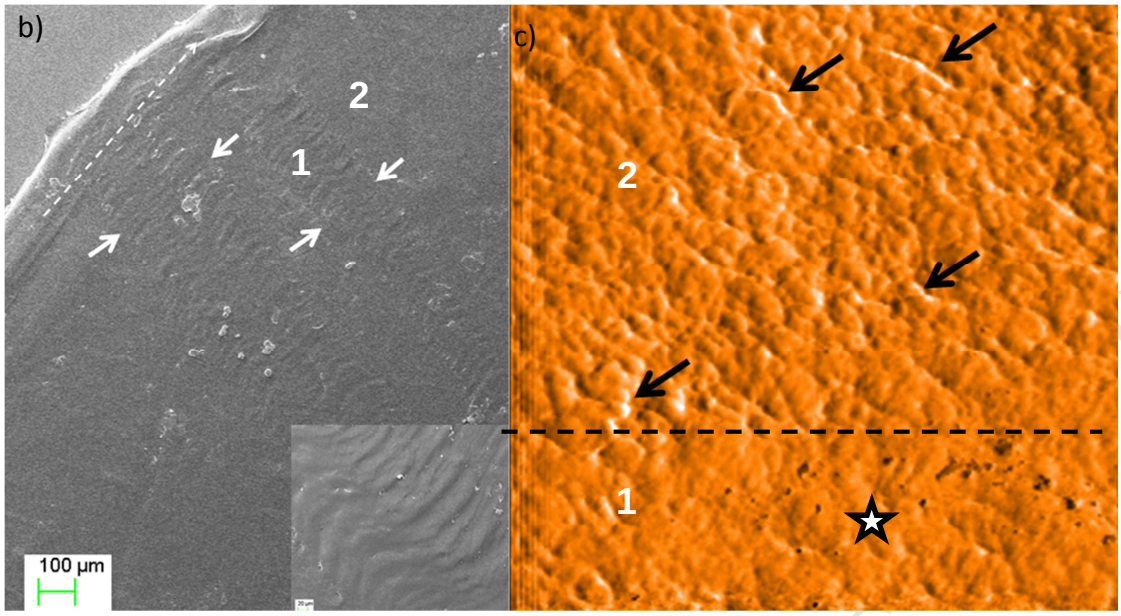

Figure 2. (a) Photographs of Parafilm/GNP film at different strains. The arrows show the formation of alternating bands with regions of low GNPs concentration. (b) FESEM images showing the formation of bands on the stretched sample. The inset shows a higher magnification view of the morphology recorded inside the band region; the dashed line in the main panel indicates the stretching direction. (c) AFM phase image (70µm x 70µm square) that is corresponding to the (1) and (2) regions of the panel (b). Black arrows indicate the presence of regions with the highest contrast in the region (2) while the asterisk indicates the microcracks. The dashed line serves to the eyes to indicate the separation between the regions (1) and (2).

The optical microscopy images recorded in reflection mode on the unstretched Parafilm/GNPs film show that GNPs once transferred to the Parafilm matrix arrange as an uninterrupted path (Fig. 3a). Electrical resistance in this sample is thus attributed to the number of such percolative GNP contacts. Electrical resistance variation of Parafilm/GNPs film as a function of the stretching ratios, λshows that the initial resistance (i. e. unstretched state) increases with stretching-ratio (Fig. 3a); the increased resistance is attributed to the reduction of percolative GNP contacts at high strains as suggested in the optical micrograph of Figs. 2a and 3a.

A different trend was observed for the Parafilm/GNP film once transferred to the fluoroelastomer substrate. As the composite film was stretched, the resistance was found to increase with the deformation, reaching a maximum value at λ_{max} (i. e. 2 and 3). Subsequently, as the specimen was brought to the initial state from λ_{max} to 1, the electrical resistance regained the initial values, suggesting an almost reversible mechanism of GNP dragging previously observed in the stretch axis direction. For the highest stretch-ratio i. e. λ_{max}=4, the resistance did not show any recovery when the sample relaxes to its un-strained condition. This is a signature that at this maximum stretch-ratio the electrical network made of GNP contacts are subjected to an irreversible deformation. Also, we did not observe any sliding of the Parafilm/GNPs film with respect to the FKM substrate in our tensile tests at macroscopic length scales as observed in Fig. 3d.Different surface deformations are however shown in FESEM images at microscopic length scale in Fig. 3e. In general, wrinkling is a sinusoidal and uniform deformation; whereas, delamination have a localized deformation; in our case, from Fig. 3e delaminations generally formed across the surface. The pre-strain, after that the delamination occurs, could be used to calculate the adhesion energy according to a model where the film can considered as an adhesive tape with pre-tension attached to a substrate [25]. From such theory of peeling for large deformations in pre-strained conditions, the pre-strain for film delamination (λ_d=4) can be expressed in terms of adhesion energy (Y), film's Young modulus (E) and film thickness (t) as $\ln(\lambda_d)=2x(Y/Ext)^{0.5}$ that for E=86MPa (calculated from the elastic region of the stress-strain curve of the Parafilm/GNPs film in Fig. 1b) and t=140μm restitutes a value for Y ~$6x10^3$N/m. This value indicates that the critical value of λ=4 found for the Parafilm/GNPs film on FKM coincides with that measured at rupture for the Parafilm/GNPs film (Fig. 1b), suggesting that FKM substrate makes reversible the Parafilm mechanical behavior until its rupture despite the plastic deformation of the Parafilm/GNPs film.

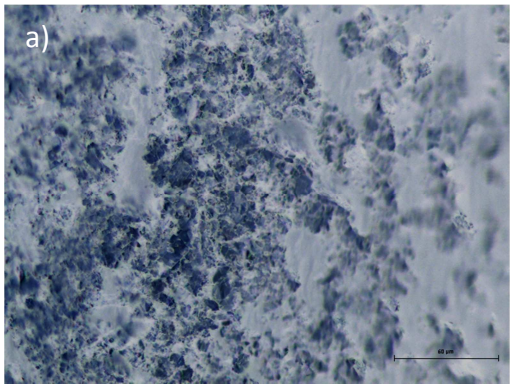
a)

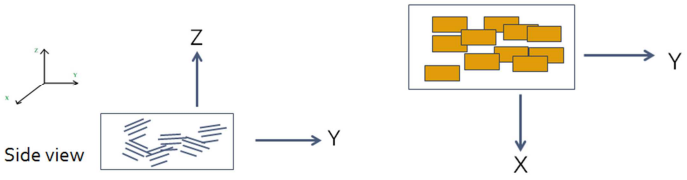
Z
Side view
Y
Y
X

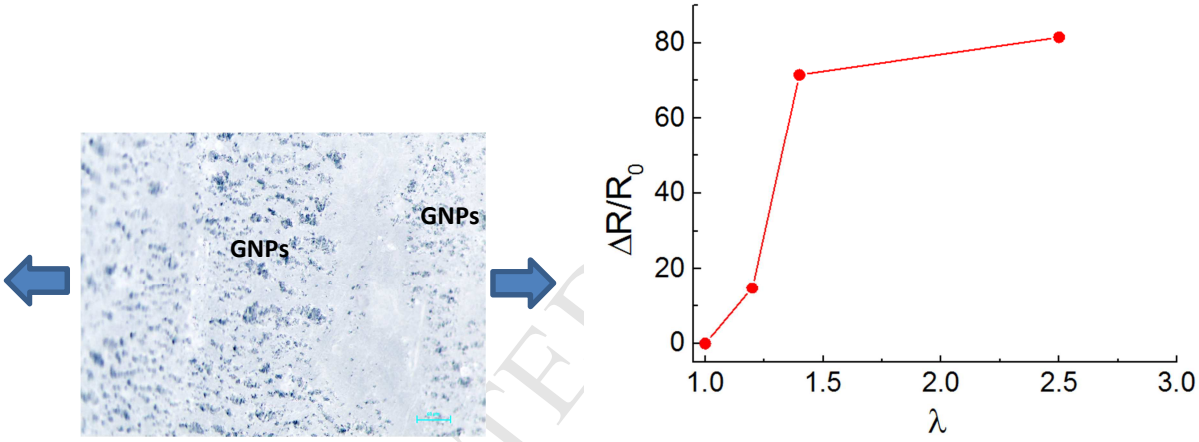
GNPs
GNPs
80
60
40
20
0
ΔR/R0
1.0
1.5
2.0
2.5
3.0
λ


Z
Side view
Y (stretched)
Top view
Y (stretched)
X

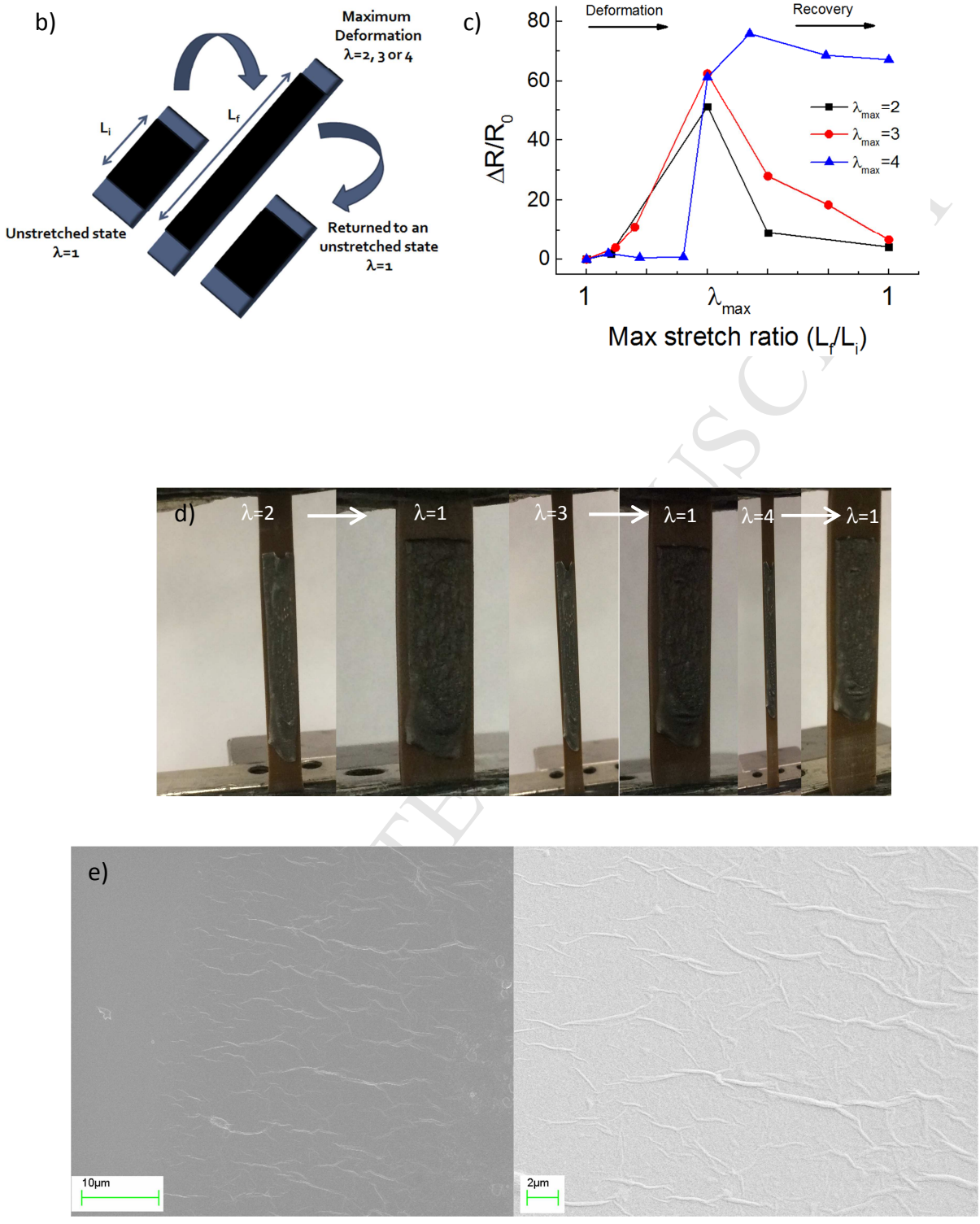

Figure 3. (a) Optical micrographs and schematic side/top view of GNP platelets embedded in Parafilm matrix in unstretched and stretched state (i. e. the arrows indicate the strain direction), respectively. The initial side/top view shows an interconnected electrical path of GNPs, GNPs then

separate during stretching, thus raising the sheet electrical resistance. (b) Schematic representation of stretch mechanism before the stretch at λ=1, during the stretch at different stretching ratios and after relaxing to an unstretched state λ=1 of Parafilm/GNPs coupled with fluoroelastomer. (c) Electrical resistance variations to initial resistance values of Parafilm/GNPs coupled with fluoroelastomer substrate through the stretching cycles from λ=1 to λ_{max}=2, 3 or 4, then returned to a relaxed state ($\lambda_{max} \rightarrow 1$). (d) Photographs of Parafilm/GNPs coupled with fluoroelastomer substrate through stretching cycle from λ=2, 3, 4 to a relaxed state (right panels). (e) FESEM images showing at different magnifications the delaminations of Parafilm/GNPs film after the stretching cycle from λ= 4 to a relaxed state.

The main drawback for practical applications of the FKM when operating in severe conditions relies on swelling and blistering caused by ethanol permeation through the thickness of the elastomeric material with a consequent lack of elasticity, poor strength and low elongation at break. On the contrary Parafilm is resistant against many polar substances, e.g. ethanol. In this regard the FKM specimen was packed with Parafilm/GNPs film and put in an oven at 110°C for 30 minutes, then the sample was cooled and immersed in ethanol for 48 hours at 25°C. For a comparison purpose a neat specimen of FKM was immersed in the same liquid. The tensile strength and ultimate elongation at the end of the required immersion period, the specimens were removed from the liquid and quickly dip in acetone and blot with filter paper. The stress-strain curves as well the mechanical characteristics of these specimens are reported in Figure 4 and Table I, respectively. The change in volume was also calculated according to the equation $(M_3\text{-}M_1)/d(M_1\text{-}M_2)\text{x}100$ where M_1 is the initial mass of the specimen in air, M_2 is the mass of the specimen immersed in distilled water at room temperature, M_3 is the mass recorded in air after the immersion in the liquid and d is the density of the immersion liquid expressed as Mg/m^3. The diffusion of the solvent depends on the concentration of free space available in the matrix which accommodates the penetration of solvent molecule [26,27]. The packaging by Parafilm/GNPs coating demonstrated a low solvent

permeability as well as the maintenance of the mechanical characteristics (see Tab. I), thus demonstrating a synergistic effect between the Parafilm/GNPs film and the FKM substrate. To assess the possible role played by GNPs on ethanol permeation through the Parafilm based coating, we report the FESEM analysis on the cross-sectional profile of the Parafilm/GNP film applied on the FKM substrate where it is clear that once laminated, the GNP are on the outer side of the Parafilm (Fig. 4b). To explain the observed barrier properties of GNPs reported in Tab. I, we recall that in general liquid (i. e. ethanol) permeation in polymer coatings occurs via a network of surface capillaries [28]. After the addition of GNPs, the top view FESEM image shows that there is a limited space left for ethanol to permeate between graphene sheets (Fig. 4b), and the only diffusion path remaining is through structural defects.

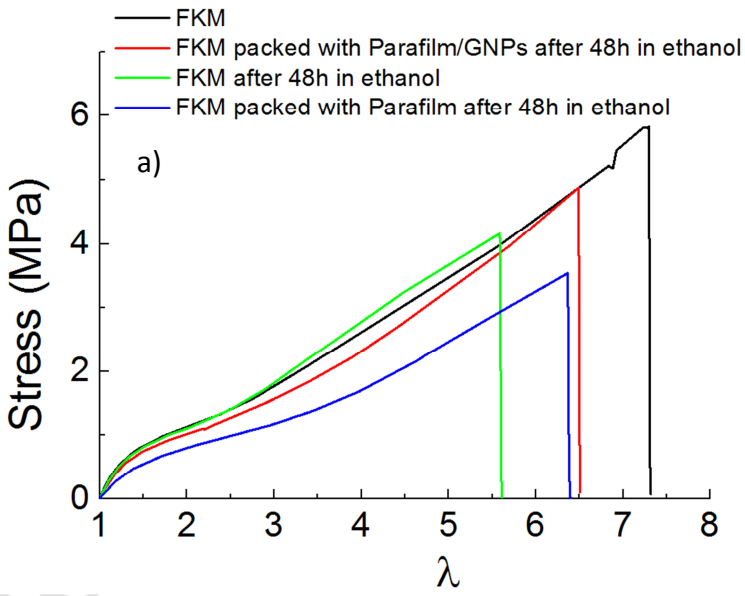

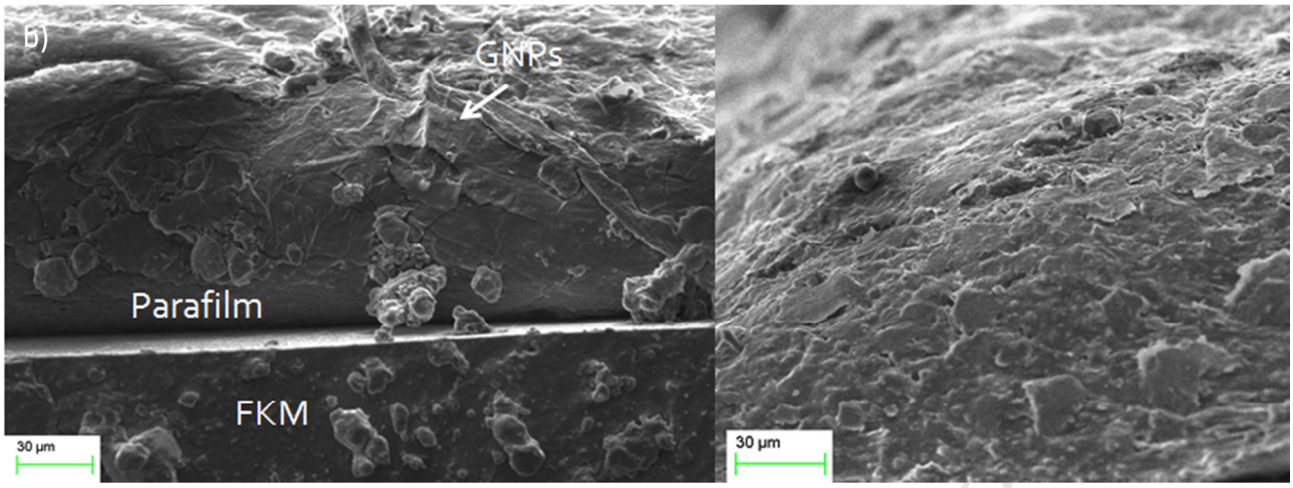

Figure 4. (a) Stress-stretch ratio curves of FKM, FKM after 48 hours of immersion in ethanol, FKM packed with Parafilm/GNPs and FKM packed with Parafilm after 48 hours in ethanol, respectively. (b) Typical cross-sectional (left panel) and top view (right panel) FESEM images of Parafilm/GNP film applied on FKM substrate.

Conclusions

We present a novel method to develop composite coatings with recoverable electrical resistance from high-strain state. The composite coating was realized from thermoplastic Parafilm commonly used in research, clinical and industrial laboratories worldwide and graphene nanoplatelets. Such materials were mechanically coupled by lamination. We also demonstrate that fluoroelastomer substrates can be used with success for the lamination transfer of such composite coatings. The GNPs in the coating creates an electrical conducting percolation network that, unlike in the Parafilm matrix, is reversible even under high strain. We found also that the Parafilm/GNPs film acts as a barrier against ethanol corrosion when applied to the FKM substrate in terms of swelling and mechanical properties. These findings suggest that future research directions in such elastomeric composite materials become possible, such as corrosion-resistant functional devices where the

solvent repellent nature of the paraffin wax coating as well as the conductivity properties when combined with conductive nanofiller adds new properties and functions to traditional elastomers.

Acknowledgements

NMP is supported by the European Research Council (ERC PoC 2015 SILKENE nr. 693670) and by the European Commission H2020 under the Graphene Flagship (WP14 “Polymer composites”, n. 696656) and under the FET Proactive (“Neurofibres” no. 732344).

References

[1] W. F. Beineke, Parafilm: new way to wrap grafts, Hortscience 13 (1978) 284–284.

[2] P. Gaskin, J. Macmilla, R. D. Firn, R. J. Pryce, Parafilm: convenient source of N-alkane standards for determination of gas chromatographic retention indices, Phytochemistry 10 (1971) 1155–1157.

[3] S. M. Higham, W. M. Edgar, Effects of parafilm and cheese chewing on human dental plaque pH and metabolism, Caries Res. 23 (1989) 42–48.

[4] J. Salamzadeh, S. Dadashzadeh, M. Habibi, S. Estifaie, Serum and saliva theophylline levels in adult outpatients with asthma and chronic obstructive pulmonary disease (COPD): a cross-sectional study, Iran. J. Pharm. Res. 7 (2008) 83–87.

[5] S. Javaherian, K. A. O'Donnell, A. P. McGuigan, A fast and accessible methodology for micro-patterning cells on standard culture substrates using parafilm (TM) inserts, PLoS ONE 6 (2011) 20909.

[6] L. G. Martins, Y. Song, T. Zeng, M. S. Dresselhaus, J. Kong, P. T. Araujo, Direct transfer of graphene onto flexible substrates, Proc. Natl. Acad. Sci. USA 110 (2013) 17762-17767.

[7] W.-L. Song, M.-S. Cao, M.-M. Lu, J. Yang, H.-F. Ju, Z.-L. Hou, J. Liu, J. Yuan, L.-Z. Fan, Alignment of graphene sheets in wax composites for electromagnetic interference shielding improvement, Nanotechnology 24 (2013) 115708.

[8] J. E. Mates, I. S. Bayer, J. M. Palumbo, P. J. Carroll, C. M. Megaridis, Extremely stretchable and conductive water-repellent coatings for low-cost ultra-flexible electronics, Nat. Commun. 6 (2015) 8874.

[9] J. Y. Woo, K. K. Kim, J. Lee, J. T. Kim, C.-S. Han, Highly conductive and stretchable Ag nanowire/carbon nanotube hybrid conductors, Nanotechnology 25 (2014) 285203.

[10] S. Yao, Y. Zhu, Nanomaterial-enabled stretchable conductors: strategies, materials and devices, Adv. Mater. 27 (2015) 1480–1511.

[11] C. F. Guo, Z. Ren, Flexible transparent conductors based on metal nanowire networks, Mater. Today 18 (2015) 143–154.

[12] P. Lee, J. Lee, H. Lee, J. Yeo, S. Hong, K. H. Nam, D. Lee, S. S. Lee, Highly stretchable and highly conductive metal electrode by very long metal nanowire percolation network, Adv. Mater. 24 (2012) 3326–3332.

[13] J. Zang, S. Ryu, N. Pugno, Q. Wang, Q. Tu, M. J. Buehler, X. Zhao, Multifunctionality and control of the crumpling and unfolding of large-area graphene, Nat. Mater. 12 (2013) 321–325.

[14] S. Rooj, A. Das, G. Heinrich, Tube-like natural halloysite/fluoroelastomer nanocomposites with simultaneous enhanced mechanical, dynamic mechanical and thermal properties, Eur. Polym. J. 47 (2011) 1746-1755.

[15] M. A. Kader, M. Y. Lyu, C. Nah, A study on melt processing and thermal properties of fluoroelastomer nanocomposites, Compos. Sci. Technol., 66 (2006) 1431-1443.

[16] T. Kuilla, S. Bhadra, D. Yao, N. H. Kim, S. Bose, J. H. Lee, Recent advances in graphene based polymer composites, Progress in Polymer Science 35 (2010) 1350–1375.

[17] A. M. Pinto, J. Cabral, D. A. Pacheco Tanaka, A. M. Mendes, F. D. Magalhaes, Effect of incorporation of graphene oxide and graphene nanoplatelets on mechanical and gas permeability properties of poly(lactic acid) films, Polym. Int. 62 (2012) 33-40.

[18] B. M. Yoo, H. J. Shin, H. W. Yoon, H. B. Park, Graphene and graphene oxide and their uses in barrier polymers, J. Appl. Polym. Sci. 131 (2014) 39628-39634.

[19] Stappers L, Yuan Y, Fransaer J. Novel composite coatings for heat sink applications. J Electrochem Soc 152 (2005) C457–61.

[20] R. Libanori, R. M. Erb, A. Reiser, H. Le Ferrand, M. J. Süess, R. Spolenak, A. R. Studart, Stretchable heterogeneous composites with extreme mechanical gradients, Nat. Commun. 3 (2012) 1265.

[21] A. R. Studart, Biological and bioinspired composites with spatially tunable heterogeneous architectures, Adv. Funct. Mater. 23 (2013) 4423–4436.

[22] C. Legge, F. Davis, G. Mitchell, Memory effects in liquid crystal elastomers, J. Phys. II 1 (1991) 1253–1261.

[23] N. Ukrainczyk, S. Kurajica, J. Šipušiæ, Thermophysical Comparison of Five Commercial Paraffin Waxes as Latent Heat Storage Materials, Chem. Biochem. Eng. Q. 24 (2010) 129–137.

[24] T. H. Ware, J. S. Biggins, A. F. Shick, M. Warner, T. J. White, Localized soft elasticity in liquid crystal elastomers, Nat. Commun. 7 (2016) 10781.

[25] N. M. Pugno, The theory of multiple peeling, Int. J. Fract. 171 (2011) 185–193

[26] W. R. Collin, W. Lewandowski, E. Schmois, J. Walish, T. M. Swager, Claisen rearrangement of graphite oxide: a route to covalently functionalized graphenes, Angew. Chem. Int. Ed. 50 (2011) 8848–8852.

[27] R. Stephen, S. Varghese, K. Joseph, Z. Oommen, S. Thomas, Diffusion and transport through nanocomposites of natural rubber (NR), carboxylated styrene butadiene rubber (XSBR) and their blends, J. Membr. Sci. 282 (2006) 162–70.

[28] B. M. Yoo, H. J. Shin, H. W. Yoon, H. B. Park, Graphene and graphene oxide and their uses in barrier polymers, J. Appl. Polym. Sci. 131 (2014) 39628-39640.